

# A Modified Anomaly Detection Method for Capsule Endoscopy Images Using Non-linear Color Conversion and Higher-order Local Auto-Correlation (HLAC)

Erzhong Hu, Hirokazu Nosato, Hidenori Sakanashi, Masahiro Murakawa

**Abstract**—Capsule endoscopy is a patient-friendly endoscopy broadly utilized in gastrointestinal examination. However, the efficacy of diagnosis is restricted by the large quantity of images. This paper presents a modified anomaly detection method, by which both known and unknown anomalies in capsule endoscopy images of small intestine are expected to be detected. To achieve this goal, this paper introduces feature extraction using a non-linear color conversion and Higher-order Local Auto Correlation (HLAC) Features, and makes use of image partition and subspace method for anomaly detection. Experiments are implemented among several major anomalies with combinations of proposed techniques. As the result, the proposed method achieved 91.7% and 100% detection accuracy for swelling and bleeding respectively, so that the effectiveness of proposed method is demonstrated.

## I. BACKGROUND

Capsule endoscopy is a pill-shaped endoscopy exploited as a patient-friendly tool in gastrointestinal examination. It is equipped with CMOS image sensors, power supply, UHF-band transmitter and LED light for illumination. Since capsule endoscopy acquired its first approval by FDA (U.S. Food and Drug Administration) in 2001, more than 1,000,000 capsules have been swallowed worldwide [1]. Capsule endoscopy examination is not real-time work, as over 50,000 images are captured and saved for further inspection [2] from one patient. This procedure usually results in a huge burden on examiners and may lead to misdiagnosis. With regard to this issue, automatic anomaly detection is deemed as a prospective assistant by identifying normal and anomaly images out of a large collection.

## II. ANOMALY DETECTION FOR CAPSULE ENDOSCOPY

Several state-of-the-art anomaly detection methods are categorized into two sorts: ‘anomaly definition’ and ‘anomaly learning’. In ‘anomaly definition’, various lesions are ruled by color components and combination beforehand. Tao Gan et al. proposed a detection method based on inspecting the color components and combination [3]. The accuracy varies from 42.9% to 91.2%. Barbara Penna et al. described and detected bleeding pixels by a certain combination of ranges in HSV color space [4]. In ‘anomaly learning’, parts of categorized anomaly images are employed for learning, with others left for testing. In the work by Baopu Li et al. [5], Tchebichef moment, Chromaticity moments and neural network was introduced for bleeding and ulcer detection. The average accuracy (specificity and sensitivity) come out around 84.68% and 92.97%.

Nevertheless, the capsule endoscopy images usually include various contents (e.g. residue, bile, lesions etc.) in multiform and mutable appearance. In some cases of ‘anomaly definition’, anomalies that do not match the definitions are very risky to be omitted. For the ‘anomaly learning’ mentioned, only one or two kinds of anomalies are able to be detected once depending on learned anomalies. This implies an enormous set of anomaly detection if detection for more kinds of anomalies is required in practical tasks.

To overcome this drawback, this paper takes advantage of our proposed anomaly detection idea [6]: Normal intestinal objects are easier to be described than ever-changing anomalies. By learning the normal and measuring the difference between testing samples and the normal, both known anomalies (foreign bodies and lesions known beforehand) and unknown anomalies are supposed to be detected all at once. On the basis of this, the proposed anomaly detection focuses on image processing and feature extraction. A non-linear conversion is introduced to improve the fineness and extend the valid range of Hue channel, combined with several fundamental techniques in image processing. Higher-order Local Auto Correlation (HLAC) [7] and its invariance transformation [8] are employed as image color features. Moreover, image partition is additionally used to find out small anomaly objects. To verify the proposed image pre-processing and feature extraction, subspace method is employed as classifier.

## III. PROPOSED ANOMALY DETECTION

The proposed anomaly detection consists of learning the normal and detecting anomalies. In accordance to this idea, learning phase and testing phase (Fig. 1) are involved.

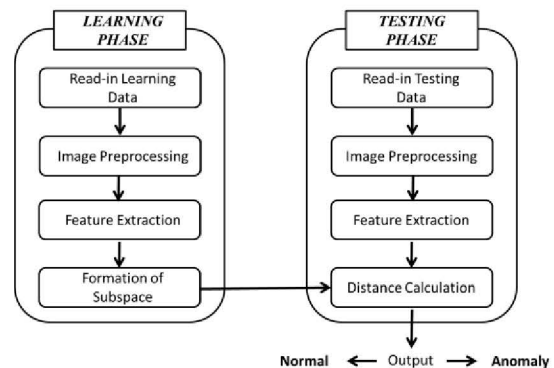


Figure 1. The proposed anomaly detection

In learning phase, images including only normal intestinal wall are employed as learning samples. After pre-processing, image features extracted from these normal images are used to establish a vector space representing the normal. Likewise, in testing phase, same features are extracted from pre-processed testing samples. Anomaly detection is in accordance with the scale of difference between testing sample and normal vector space. In the following statement, brightness filter and non-linear Color Conversion are for image pre-processing; HLAC and image partition constitute feature extraction. Subspace is referred at last.

#### A. Brightness Filter

In the captured images, lumen regions usually show lower brightness and objects in this region are uninformative. As the first step of image pre-processing, a brightness filter is utilized as (1). Such uninformative pixels are excluded (Fig.2).

$$\begin{cases} R = G = B = 0 \\ \text{(if } 0 \leq 0.299R + 0.587G + 0.114B \leq 55) \\ \text{No change} \\ \text{(if } 55 < 0.299R + 0.587G + 0.114B \leq 255) \end{cases} \quad (1)$$

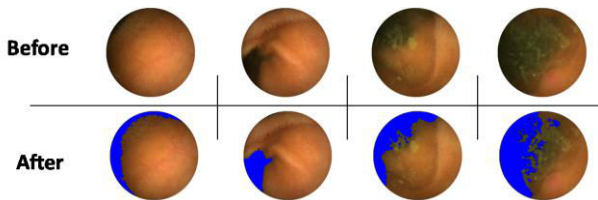


Figure 2. Brightness filter

#### B. Non-linear Color Conversion

HSV is an intuitive color space with Hue channel independently indicating difference between various colors corresponding to the wavelength of color. For capsule endoscopy images, various contents (residue, swelling etc.) represented in Hue channel are distinguishable by human's color perception. Meanwhile, hue channel is hardly affected by illumination condition. Hue channel is employed alone in proposed method.

Fig. 3 is an example of distribution of Hue components in one patient's images (screened by brightness filter). Overwhelming majority of non-zero components span the range [0, 72], leaving almost no other components outside this range (proportion of components within (72, 360) is smaller than  $2 \times 10^{-8}$ ). Such narrow region leads to an issue that number of components is small in the region with very limited numerical difference among them.

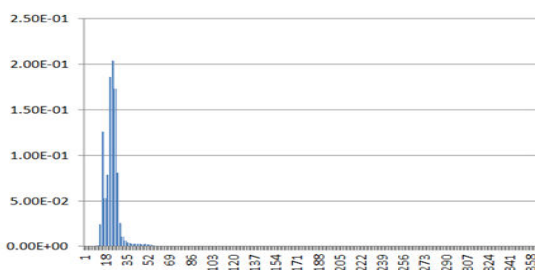


Figure 3. Hue components in ordinary capsule endoscopy images

To improve the precision and extend the valid range of Hue channel, so that numerical difference between components are able to more effectively reflected by image features, a unique conversion is proposed in this paper. The conversion is indicated as the following formula:

$$\text{Hue}_{\text{after}} = \begin{cases} 0 & \text{(if } \text{Hue}_{\text{before}} = 0 \text{ or } 80 < \text{Hue}_{\text{before}} \leq 360) \\ 360 & \text{(if } 0 < \text{Hue}_{\text{before}} \leq 10) \\ 1.0877^{(80 - \text{Hue}_{\text{before}})} & \text{(if } 10 < \text{Hue}_{\text{before}} \leq 80) \end{cases} \quad (2)$$

After conversion, the histogram of images is depicted as Fig. 4. With the Hue components extended to a much wider range, difference of neighboring components is amplified accordingly.

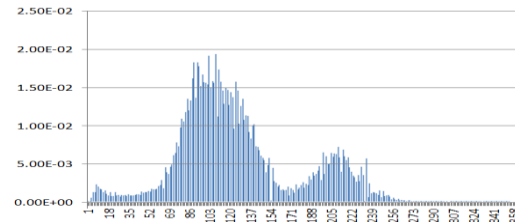


Figure 4. Hue components in converted capsule endoscopy images

#### C. Feature Extraction

Higher-order Local Auto-Correlation (HLAC) [7] has been demonstrated as an effective image feature for capsule endoscopy images [6]. Besides, it also successfully applied in many applications such as counting objects [9] and anomaly detection for pathological images [8], are adopted in feature extraction. HLAC features possess 'shift invariance', which indicates no impact on HLAC features wherever intestinal contents are located within the image. Meanwhile, the property that only sum-of-product calculation is executed provides extraction process of large number of images captured by capsule endoscopy with very low computational cost. Besides, HLAC features are robust against single-pixel noise commonly occurring in capsule endoscopy images. The N-th order HLAC is described as following autocorrelations:

$$R_N(\mathbf{a}_1, \dots, \mathbf{a}_N) = \sum_{\mathbf{r}} I(\mathbf{r})I(\mathbf{r} + \mathbf{a}_1) \cdots I(\mathbf{r} + \mathbf{a}_N) \quad (3)$$

where  $I$  is an objective gray-scale image,  $\mathbf{r}$  is a position vector, and  $\mathbf{a}_i$  indicates the displacement vector. Equation (3) takes many forms by varying the order  $N$ . Taking the balance of effectiveness and computational burden into consideration, this paper adopts  $N \in \{0, 1, 2\}$ . In this situation, HLAC features are expressed by 35 mask patterns and constitute a 35-dimensional vector. Moreover, capsule endoscopy passes through gastrointestinal tract with ruleless movement and rotation all along. Since rotation and inversion make no contribute to anomaly detection, patterns in same shape and different directions are put into same group [8]. By this means, the 35-dimension vectors are further restructured to 8-dimension vectors.

#### D. Image Partition

In feature extraction, HLAC features are obtained on the coverage of whole image so that small local lesions make limited contribution to be reflected in feature vectors. With this issue concerned, this paper additionally adopts image partition to detect anomaly in small local regions. One image is divided into 16 subareas. With both universal coverage and

computational cost considered, each 2×2 subareas are regarded as a larger subarea. In this way, 9 subareas (Fig.5) are generated for independent feature extraction and anomaly detection.

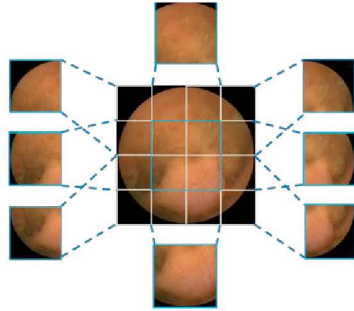


Figure 5. 9 subareas by image partition

### E. Subspace Method

Subspace method [10] is broadly used in 2-way classification. In this paper, it is employed to form a normal subspace and detect anomalies. Suppose there is a set of normal sample vectors  $\{X_1, X_2 \dots X_R\}$ , containing  $M$ -dimension vectors of  $R$  learning images. The eigenvectors  $U=[u_1, u_2, \dots, u_M]$  of the autocorrelation matrix of  $X$  are obtained as:

$$U^T C U = \Lambda \quad (4)$$

where  $\Lambda = \text{diag}(\lambda_1, \lambda_2, \dots, \lambda_S)$  is the eigenvalue matrix.  $C$  is the autocorrelation matrix of  $X$ . The order  $K$  of the normal subspace is calculated according to the contribution rate  $\eta_K$  described in (5). If  $\eta_K$  exceeds a certain threshold (0.99, 0.999...) with a smallest  $K=K_1$ , the order is set as  $K_1$ .

$$TH \leq \eta_K = \frac{\sum_{i=1}^K \lambda_i}{\sum_{i=1}^M \lambda_i} \quad (5)$$

And next, with the order  $K_1$ , normal subspace  $U_{K_1} U_{K_1}^T$  is formed based on the eigenvectors  $U_K = \{u_1, \dots, u_{K_1}\}$ . The distance  $d_{\perp}$  between feature vector  $x$  extracted from test image and the normal subspace is defined as:

$$d_{\perp} = x^T (I_M - U_K U_K^T) x \quad (6)$$

where  $I_M - U_K U_K^T$  ( $I_M$  is the  $M$ -dimension identity matrix) indicates the ortho-complement subspace of normal subspace. In term of higher anomaly degree indicated by larger deviation distance, test images or subareas are deemed to be anomaly with deviation distances larger than a pre-set threshold  $T$  (stated in IV. B).

## IV. EXPERIMENTS

### A. Capsule Endoscopy Image Data

Capsule endoscopy images (Fig.6) are derived from two patients' video and each of them are selected and tagged by an experienced doctor beforehand. The principle for discriminating normal and anomaly could be interpreted as whether the contents belong to normal intestinal organ. Swelling and bleeding are very common intestinal symptoms. Beside, though residues (food, drugs and bile) do not represent any kind of disease, they sometimes emerge with lesions

simultaneous so that they regarded as potential risk and detected as anomaly.

TABLE I. CAPSULE ENDOSCOPY IMAGES USED IN EXPERIMENTS.

|           | Normal wall and lumen |              | Residue | Swelling | Bleeding |
|-----------|-----------------------|--------------|---------|----------|----------|
|           | wall                  | lumen        |         |          |          |
| Patient 1 | 523 (images)          |              | 120     | 458      |          |
|           | Learning: 354         | Testing: 169 |         |          |          |
| Patient 2 | 266                   |              | 250     |          | 310      |
|           | Learning: 166         | Testing: 100 |         |          |          |

Images of each patient are divided into two sets: learning set and testing set. In accordance to the anomaly detection principle, 354 and 166 learning images of patient 1 and 2 includes only normal intestinal wall and lumen, with all the other images remained for testing. (Table I)

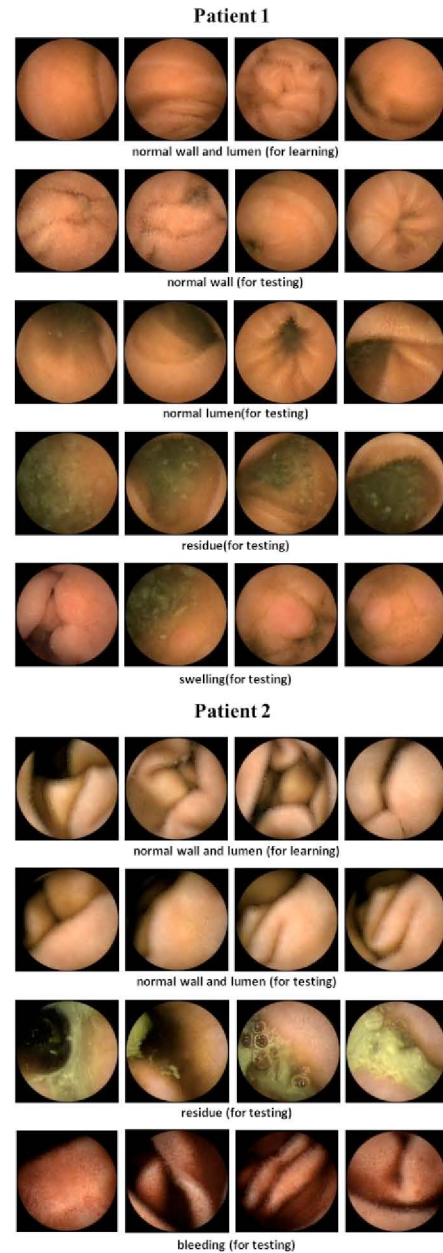


Figure 6. Examples of images from patient 1 and 2.

## B. Experimental Results

In order to demonstrate the efficacy of the proposed image processing and image partition, proposed anomaly detections method are conducted, by 4 methods (Table II) of different combinations of technique elements.

TABLE II. ANOMALY DETECTIONS IN 4 GROUPS.

|          | Non-linear Color conversion | Image division |
|----------|-----------------------------|----------------|
| Method 1 | ×                           | ×              |
| Method 2 | ○                           | ×              |
| Method 3 | ×                           | ○              |
| Method 4 | ○                           | ○              |

The threshold  $T$  for anomaly detection is determined by the mean  $\mu$  and standard deviation  $\sigma$  of the deviation distances between all the learning images' feature vectors and the normal subspace by these images themselves. According to these distances,  $T$  is set as  $T = \mu + 3\sigma$ . In addition, entirely dark images or subareas will be rejected to detect and categorized as anomaly.

Sensitivity and specificity, which are widely used to evaluate the performance of classification, are employed in this paper. The definitions are given as the following:

$$\text{Sensitivity} = \frac{\text{Number of correct positive predictions}}{\text{Number of positives}} \quad (7)$$

$$\text{Specificity} = \frac{\text{Number of correct negative predictions}}{\text{Number of negatives}} \quad (8)$$

Statistical results of sensitivity and specificity by the proposed method are denoted below.

TABLE III. STATISTICAL RESULTS OF SENSITIVITY.

|           |          | Residue        | Swelling       | Bleeding      |
|-----------|----------|----------------|----------------|---------------|
| Patient 1 | Method 1 | 100%(120/120)  | 70.7%(324/458) | -             |
|           | Method 2 | 100%(120/120)  | 75.3%(345/458) | -             |
|           | Method 3 | 100%(120/120)  | 12.9%(59/458)  | -             |
|           | Method 4 | 100%(120/120)  | 91.7%(420/458) | -             |
| Patient 2 | Method 1 | 98%(245/250)   | -              | 100%(310/310) |
|           | Method 2 | 95.2%(238/250) | -              | 100%(310/310) |
|           | Method 3 | 96.4%(241/250) | -              | 100%(310/310) |
|           | Method 4 | 93.6%(234/250) | -              | 100%(310/310) |

TABLE IV. STATISTICAL RESULTS OF SPECIFICITY

|           |          | Normal wall and lumen |                |
|-----------|----------|-----------------------|----------------|
|           |          | Wall                  | Lumen          |
| Patient 1 | Method 1 | 100%(169/169)         | 95.6%(241/252) |
|           | Method 2 | 88.1%(149/169)        | 100%(252/252)  |
|           | Method 3 | 100%(169/169)         | 96.4%(243/252) |
|           | Method 4 | 91.1%(154/169)        | 98.4%(248/252) |
| Patient 2 | Method 1 | 100%(100/100)         |                |
|           | Method 2 | 91%(91/100)           |                |
|           | Method 3 | 99%(99/100)           |                |
|           | Method 4 | 100%(100/100)         |                |

As the result of sensitivity (Table III), Method 4 using both proposed color conversion and image partition shows most effectiveness in swelling detection. The accuracy is raised up from 70.7% to 91.7%. This is easily owed to the reason that

color space conversion makes reddish components more dominant. In bleeding detection, four groups all achieve 100% accuracy. Compared with swelling, bleeding usually shows stronger redness and this specialty is more explicitly reflected in both ordinary and converted Hue channel. High specificities from normal images by 4 methods indicate well restrained false positive (normal images detected as anomaly). Either of them achieves remarkable accuracy with most of normal images correctly recognized. Likewise, as depicted in Table IV, there is no noteworthy difference in residue detection.

## V. CONCLUSION

Aiming to lower the workload of capsule endoscopy examiners, this paper presents an anomaly detection method, in which a non-linear color conversion and Higher-order Local Auto Correlation (HLAC) are introduced for feature extraction. Combined with other brightness filter and image partition, anomaly detection is realized by subspace method. Evaluation of performance is implemented on four types of intestinal contents from two patients. As denoted in statistical results, both outstanding specificity and sensitivity are validated.

## ACKNOWLEDGMENT

Gratitude is expressed to Yasuo Suzuki M.D. and Hiroshi Aoki M.D. at Toho Univ. Sakura Medical Center, for collecting and providing the capsule endoscopy video data and attaching tags to them.

## REFERENCES

- [1] Zvi Fireman, 'Capsule endoscopy: Future horizons', World Journal of Gastrointestinal Endoscopy, Sep 16 (2010), 2(9):305-307.
- [2] M. Delvaux, Capsule endoscopy: techniques and indications, Best Practice & Research Clinical Gastroenterology, 22 (5) (2008), pp. 813-837.
- [3] Tao Gan, Jun-Chao Wu, Ni-Ni Rao, Tao Chen, Bing Liu, A feasibility trial of computer-aided diagnosis for enteric lesions in capsule endoscopy, World Journal of Gastroenterology, 2008 December 7, 14(45), 6929-6935.
- [4] Barbara Penna, Tammam Twello et al., 'A Technique for Blood Detection In Wireless Capsule Endoscopy Images', 17th European Signal Processing Conference (EUSIPCO 2009), pp. 1865-1868.
- [5] Baopu Li, Max Q.-H. Meng, Computer-based detection of bleeding and ulcer in wireless capsule endoscopy images by chromaticity moments, Computers in Biology and Medicine 39 (2009) 141-147
- [6] Erzhong Hu, Hirokazu Nosato, Hidenori Sakanashi, Masahiro Murakawa, 'Anomaly Detection for Capsule Endoscopy Images Using Higher-order Local Auto Correlation Features', 2012 IEEE International Conference on Systems, Man, and Cybernetics (SMC 2012), Oct. 2012, pp. 2289- 2293
- [7] N. Otsu and T. Kurita, 'A new scheme for practical flexible and intelligent vision systems', Proc. IAPR Workshop on Computer Vision, 1988, pp. 431-435.
- [8] Hirokazu Nosato, Tsukasa Kurihara, Hidenori Sakanashi, Masahiro Murakawa et al., 'An extended method of Higher-order Local Autocorrelation feature extraction for classification of histopathological images', IPSJ Transactions on Computer Vision and Applications, Dec. 2011, Vol.3 211-221.
- [9] Takumi Kobayashi, Tadaaki Hosaka et al., 'HLAC approach to automatic object counting, Bio-inspired', Learning and Intelligent Systems for Security, 2008, 40-45.
- [10] Takuya Nanri and Nobuyuki Otsu, 'Unsupervised Abnormality Detection in Video Surveillance', Proc. IAPR Conf. on Machine Vision Application, 2005, pp. 574-577